npg

ORIGINAL ARTICLE

Bacterial colonization of *Hydra* hatchlings follows a robust temporal pattern

Sören Franzenburg[1,4], Sebastian Fraune[1,4], Philipp M Altrock[2], Sven Künzel[2],
John F Baines[2,3], Arne Traulsen[2] and Thomas CG Bosch[1]

[1]*Zoological Institute, Christian-Albrechts University Kiel, Kiel, Germany;* [2]*Max-Planck-Institute for Evolutionary Biology, August-Thienemann-Straße 2, Plön, Germany and* [3]*Institute for Experimental Medicine, Christian-Albrechts-University of Kiel, Kiel, Germany*

Animals are colonized by complex bacterial communities. The processes controlling community membership and influencing the establishment of the microbial ecosystem during development are poorly understood. Here we aimed to explore the assembly of bacterial communities in *Hydra* with the broader goal of elucidating the general rules that determine the temporal progression of bacterial colonization of animal epithelia. We profiled the microbial communities in polyps at various time points after hatching in four replicates. The composition and temporal patterns of the bacterial communities were strikingly similar in all replicates. Distinct features included high diversity of community profiles in the first week, a remarkable but transient adult-like profile 2 weeks after hatching, followed by progressive emergence of a stable adult-like pattern characterized by low species diversity and the preponderance of the Betaproteobacterium *Curvibacter*. Intriguingly, this process displayed important parallels to the assembly of human fecal communities after birth. In addition, a mathematical modeling approach was used to uncover the organizational principles of this colonization process, suggesting that both, local environmental or host-derived factor(s) modulating the colonization rate, as well as frequency-dependent interactions of individual bacterial community members are important aspects in the emergence of a stable bacterial community at the end of development.

Introduction

All animals, ranging from simple invertebrates to primates, are host to complex microbial communities (Fraune and Bosch, 2007; Ley *et al.*, 2008; Ochman *et al.*, 2010). Microbial colonization appears to be an essential step in vertebrate ontogeny, contributing to the maturation of the immune system and gut development (Rawls *et al.*, 2004; Mazmanian *et al.*, 2005; Kelly *et al.*, 2007). Resident gut bacteria can cause disease if the balance of the community is disrupted by antibiotics (Ayres *et al.*, 2012). Neonatal recolonization of germ-free mice with microbes prevents enhanced colitis and asthma sensitivity while exposure of adult mice to these conditions is not effective (Olszak *et al.*, 2012). In invertebrates, germ-free *Drosophila* larvae show drastically increased mortality compared with

conventional larvae when reared on a nutrient-poor diet (Shin *et al.*, 2011); and in anthozoan cnidarians shifts in the composition of the microbial community are associated with coral bleaching (Mao-Jones *et al.*, 2010). Thus, vertebrates and invertebrates appear not only to tolerate, but to require colonization by beneficial microorganisms for metabolism, immune defense, development, behavior (Sandstrom *et al.*, 2000; Xu *et al.*, 2003; Nyholm and McFall-Ngai, 2004; Rawls *et al.*, 2004; Mazmanian *et al.*, 2005; Chow *et al.*, 2010) and most likely many other not yet identified functions. Any animal with its associated microbes, therefore, can be considered as a metaorganism defined as 'an ensemble of individuals representing numerous species that coexist and interact in an area or habitat' (Drake, 1990). Membership in such a community is frequently influenced by interactions among species and properties, which emerge from such interactions (Drake, 1990). In this sense, humans develop into ecological communities after being born with a sterile gastrointestinal tract that is successively colonized with microbial populations until adult-like communities stabilize (Koenig *et al.*,

2011; Walter and Ley, 2011). The processes, which control community membership in the neonatal gut and influence the colonization pattern during infancy and childhood are poorly understood. A vitally important question to ask, therefore, is what are the factors and rules in a particular host that influence community assembly, composition and diversity. Because a dysregulation of host–microbe homeostasis can have severe impact on the host's health, controlling and mediating 'correct' bacterial colonization in early life would confer fitness advantages to the host. This view has encouraged discussions as to what extent the microbiota is controlled by the host through top–down mechanisms involving the immune system, relative to microbiota intrinsic bottom–up mechanisms (Ley *et al.*, 2006). Despite the importance of understanding the factors that control bacterial colonization in man, however, the inaccessibility of the microbial niches of the human gut, and the restriction of studies in infants to collection of fecal samples (Cilieborg *et al.*, 2012) make it desirable to use animal models for understanding basic principles of colonization processes in detail. Here we aimed to explore the assembly of bacterial communities in the freshwater polyp *Hydra*. Our goal was to obtain mechanistic information about specific host–bacterial interactions and to elucidate the rules that determine how large and diverse bacterial populations colonize a newly born animal.

The cnidarian *Hydra* is an established animal model for studying host–microbe interactions. It is inexpensive, easily handled, has a transcriptome and genome that more closely resembles humans than those of flies and worms (Chapman *et al.*, 2010; Hemmrich *et al.*, 2012), and is colonized by stable and species-specific bacterial communities (Fraune and Bosch, 2007). Unlike most animal systems, it is possible to examine temporal bacterial profiles of clonal lineages without being limited to fecal samples, as *Hydra* grows clonally under constant laboratory conditions. *Hydra*'s tube-like body (Figure 1a) resembles in several aspects the anatomy of the vertebrate intestine with the endodermal epithelium lining the gastric cavity and the ectodermal epithelium providing a permanent protective barrier to the environment (Bosch, 2012). Changes in *Hydra*'s epithelial homeostasis cause significant changes in the microbial community (Fraune *et al.*, 2009), implying a direct interaction between epithelia and microbiota. Multifunctional epithelial cells recognize microbial-associated molecular patterns with the help of the Toll-like receptor signaling pathway (Bosch *et al.*, 2009; Franzenburg *et al.*, 2012). Intracellular recognition of bacteria in *Hydra* is supposed to be mediated by a large number of nucleotide oligomerization domain-like receptors (Lange *et al.*, 2011). Prominent effector molecules downstream of the conserved Toll-like receptor cascade are antimicrobial peptides.

Following fertilization, *Hydra* oocytes develop by a radial cleavage pattern outside the female polyp (Figure 1a) (Martin *et al.*, 1997). Gastrulation is followed by a cuticle stage, which is characterized
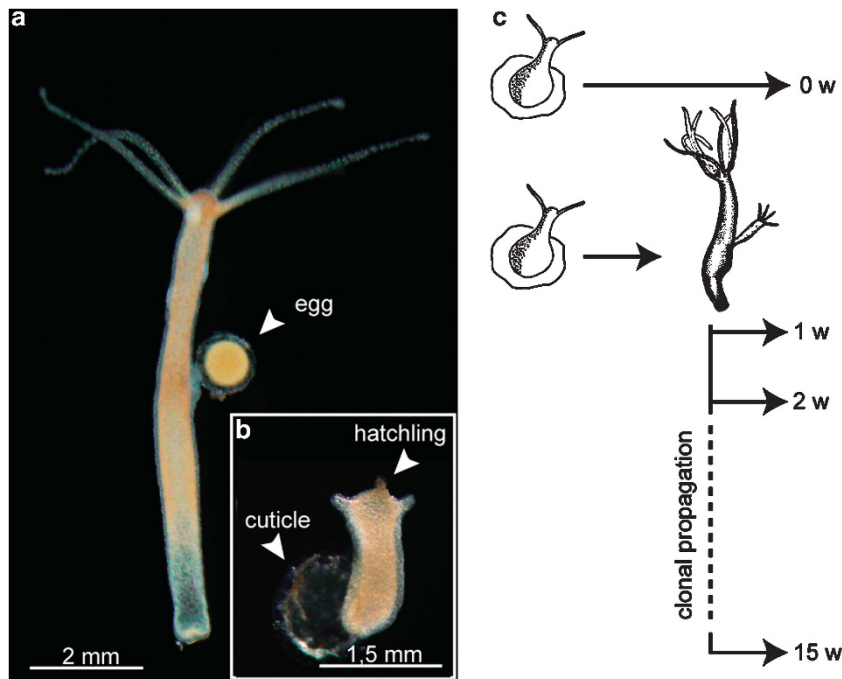

Figure 1 *Hydra* morphology and experimental design. (**a**) Female polyp of *Hydra vulgaris* (AEP) with a developing embryo. (**b**) *Hydra* hatchling eclosing from the cuticle. (**c**) Experimental design: First batch of hatchlings was used for immediate DNA extraction. Second batch of hatchlings was used for the establishment of clonal cultures, from which one polyp was removed for DNA extraction every week until week 15. Subsequently, the bacterial communities of these samples were determined by 454 sequencing.

by a thick protective outer layer (Martin *et al.*, 1997). We have shown previously (Fraune *et al.*, 2010) that early embryonic stages before the cuticle stage are colonized by a limited number of microbes, which are clearly distinct from later developmental stages. Interestingly, the differential colonization is reflected in differences in antimicrobial activity (Fraune *et al.*, 2010). Young *Hydra* polyps directly hatch from the cuticle stage (Figure 1b) (Martin *et al.*, 1997). To elucidate how bacterial communities assemble in newly hatched *Hydra* polyps, we profiled the composition of the microbiota in polyps over the first 15 weeks after hatching (Figure 1c) using culture-independent pyrosequencing of bacterial DNA. The surprisingly dynamic, but robust bacterial succession pattern prompted us to include a mathematical modeling approach to infer organizational principles that may influence community assembly and diversity. To this end, we identified the minimally required principles to model the observed bacterial succession pattern during colonization mathematically.

Materials and methods

Animals
Experiments were carried out using *Hydra vulgaris* (strain AEP) (Hemmrich *et al.*, 2007). Female polyps were induced to sexual reproduction by reduced feeding (Wittlieb *et al.*, 2006). Detached eggs were collected and separated into single wells. Eggs were screened daily for hatched polyps. After 2 weeks, first eclosed polyps were stored at − 20 °C. Next, clonal cultures were established using four hatchlings eclosed on the same day. All animals were cultured under constant, identical environmental conditions including culture medium, food (first-instar larvae of *Artemia salina,* fed three times per week) and temperature according to standard procedures (Lenhoff and Brown, 1970). One week post hatching, the first bud detached from the founder polyp and was frozen for later sequencing. Subsequently, one polyp of each clonally aging culture was removed and frozen every week until 15 weeks post eclosion.

DNA extraction and sequencing of 16S rRNA genes
For total DNA extraction, single polyps were subjected to the DNeasy Blood & Tissue Kit (Qiagen, Hilden, Germany) after being washed three times with sterile filtered culture medium. Extraction was performed following the manufacturer's protocol, except that DNA was eluted in 50 µl. For sequencing of the bacterial 16S rRNA genes, the variable regions 1 and 2 (V1V2) were amplified using the universal forward primer V2_B_Pyro_27F (5′-CTATGCGCCTTGCCAGCCCGCTCAG*TC*AGAGTT TGATCCTGGCTCAG-3′) which consists of the 454 FLX Amplicon primer B, a two base linker and the

universal 16S primer 27F and the barcoded reverse primer V2_A_338R (5′-CGTATCGCCTCCCTCGCGCCA TCAGNNNNNNNNNNN*CA*TGCTGCCTCCCGTAGGA GT-3′) which contains the 454 FLX Amplicon primer A, a sample-specific 10-mer barcode (N's), a two base linker and the universal 16S primer 338R. Twenty-five microlitre PCR reactions were performed using the Phusion Hot-Start II DNA polymerase (Finnzymes, Espoo, Finland) following the manufacturer's instructions. PCR conditions consisted of an initial denaturation step (98 °C, 30 s) followed by 30 cycles of denaturation (98 °C, 9 s), annealing (55 °C, 30 s) and elongation (72 °C, 20 s). PCR was terminated by a final elongation of 72 °C for 10 min. All reactions were performed in duplicates, which were combined after PCR. PCR products were extracted from agarose gels with the Qiagen MinElute Gel Extraction Kit (Hilden, Germany) and quantified with the Quant-iT dsDNA BR Assay Kit (Invitrogen, Calsbad, CA, USA) on a NanoDrop 3300 Fluorometer. Equimolar amounts of purified PCR product were pooled and further purified using Ampure Beads (Agencourt, Brea, CA, USA). A sample of each library was run on an Agilent (Santa Clara, CA, USA) Bioanalyzer before emulsion PCR and sequencing as recommended by Roche (Penzberg, Germany). Amplicon libraries were subsequently sequenced on a 454 GS-FLX (Roche) using Titanium sequencing chemistry.

16S rRNA 454 analysis
16S rRNA amplicon sequence analysis was conducted using the Qiime 1.3.0 package (Caporaso *et al.*, 2010). Using the sequence fasta-file, a quality file and a mapping file which assigned the 10-nucleotide barcodes to the corresponding sample as input, the sequences were analyzed using the following parameters: length between 300 and 400 bp, no ambiguous bases and no mismatch to the primer sequence. Chimeric sequences were identified and removed using Chimera Slayer (Haas *et al.*). Resulting high-quality reads ranged from 2110 to 9845 per sample. Sequences were normalized to 2000 sequences per sample, grouped into operational taxonomic units (OTUs) at a ⩾ 97% sequence identity threshold and classified by ribosomal database project (RDP) classifier. Alpha diversity was calculated using the Chao1 metric implemented in Qiime. Beta diversity was assessed using Pearson's distance (1000 replicates). A total of 454 data are deposited at MG-RAST (id: 1706).

Quantification of bacterial 16S genes by quantitative reverse transcriptase-PCR
Total bacterial quantification was performed with the original DNA used for 454 sequencing using the QuantiTect Probe RT-PCR Kit (Qiagen) and a 7300 real-time PCR system (ABI, Foster City, CA, USA). Template amounts were equilibrated for the

Hydra actin gene (hyActinF 5′-GAATCAGCTG
GTATCCATGAAAC-3′ and hyActinR 5′-AACAT
TGTCGTACCACCTGATAG-3′). Samples were nor-
malized to 15 weeks post hatching. Bacterial DNA
was quantified with universal bacteria primers
Eub341_F and Eub534_R (Muyzer *et al.*, 1993). The
fold change was calculated using the formula fold
change $= 2^{-\Delta\Delta Ct}$ with Ct being the PCR threshold
cycle.

Mathematical modeling
The mathematical basis of our model is the
replicator-mutator equation, which describes the
dynamics of different types in a competitive envir-
onment based on pairwise interactions. In our case,
a colonization rate reintroducing bacterial types
corresponds to mutations. We assumed that the
number of types is fixed. The rate of change of a
type's relative abundance is proportional to its
fitness, relative to the fitness averaged across all
types. Competition means that a type that performs
better than average increases in relative abundance.
If it performs worse, it will decrease in relative
abundance. The fitness of each type is either
constant or depends on interactions with other
types (frequency-dependent fitness). We also sought
to maintain a minimum diversity irrespective of the
performance in competition, which is modeled by a
colonization rate: For each type, the relative abun-
dance increases at the expense of an equally
distributed decrease of all other types.

The bacterial types were labeled with i ($i = 1, ..., n$).
A type's relative abundance is denoted by x_i, its
change over time (as a derivative with respect to
time) is $\dot{x}_i$. All relative abundances sum up to
one. The fitness of a type is denoted f_i. Fitness
can be constant or frequency-dependent. The
average fitness across all bacterial types is
$\bar{f} = x_1 f_1 + x_2 f_2 + ... + x_n f_n$. Owing to colonization, the
rate at which the abundance of a type increases at the
expense of other types is $\lambda/(n-1)$, multiplied with
the average fitness of all other types, $\bar{f}_i^r = \bar{f} - x_i f_i$. The
colonization rate can be time-dependent, $\lambda(t)$, and
corresponds to a mutation rate. The dynamics are
governed by the following equation:

$$\dot{x}_i = x_i\left(f_i - \bar{f}\right) + \lambda(t)\left(\frac{\bar{f}_i^r}{n-1} - x_i f_i\right)$$

The first term describes change due to the differ-
ence to the average performance of the bacterial
community. The second term describes random gain
from, and loss to all other types proportional to the
rate of colonization. The fitness of each type can
either be a constant, $f_i = w_i$, or frequency-dependent
$f_i = a_{i1}x_1 + a_{i2}x_2 + a_{i3}x_3 + a_{i4}x_4$, where a_{ik} is the para-
meter for species i interacting with species k. For our
numerical example in Figure 5c, constant selection,
we used $\{w_1, w_2, w_3, w_4\} = \{0.1, 0.4, 1.0, 0.6\}$.

In Figures 5d and e, frequency-dependent selec-
tion, we used:

$$\begin{pmatrix} a_{11} & a_{12} & a_{13} & a_{14} \\ a_{21} & a_{22} & a_{23} & a_{24} \\ a_{31} & a_{32} & a_{33} & a_{34} \\ a_{41} & a_{42} & a_{43} & a_{44} \end{pmatrix} = \begin{pmatrix} 0.20 & 0.85 & 0.95 & 0.05 \\ 0.05 & 0.90 & 0.35 & 0.80 \\ 0.35 & 0.10 & 0.10 & 0.75 \\ 0.55 & 0.35 & 0.35 & 0.35 \end{pmatrix}$$

In Figures 5c and d the colonization rate was
constant, $\lambda = 0.02$, in Figure 5e it was time-depen-
dent according to $\lambda(t) = 0.02 e^{-t/20}$. Note that the
parameter choices are for illustration only, it does
not represent a fit to the *Hydra* system.

Results

*Bacterial population profiles in newly hatched Hydra
polyps*
To follow the assembly of the microbiota in newly
hatched polyps, we established four clonal cultures
(that is, four replicates) of single hatchlings and
examined them for up to 15 weeks (Figure 1c). The
composition of the microbiota was determined by
pyrosequencing of the variable regions 1 and 2
(V1V2) of the bacterial 16S rRNA gene, amplified
from total DNA extractions of single polyps. Pyr-
osequencing resulted in 1 77 862 high-quality reads
ranging from 2110 to 9845 reads per sample. For
inter-sample comparisons, the number of reads was
normalized to 2000 reads per sample. In all four
replicates, comprising bacterial profiles of a total of
36 polyps, bacterial species estimation using the
Chao1 metric showed the highest bacterial diversity
immediately after hatching (black line, Figure 2).
About 350 different OTUs (97% sequence similarity)
were estimated in polyps just emerging from the
cuticle stage. In all four replicates, bacterial diver-
sity decreased in the following 2–3 weeks to about
150 OTUs. Thereafter, 4 weeks post hatching, a
transient but distinct increase in bacterial diversity
to 200–300 OTUs per polyp was observed (Figure 2),
followed by a decrease in bacterial diversity in all
four replicates to ~100 OTUs per polyp 15 weeks
post hatching. Thus, the diversity of the bacterial
community in *Hydra* polyps at various time points
after hatching is negatively correlated with devel-
opmental age (see also Supplementary Figure S1A).

To examine whether the changes in bacterial
diversity are accompanied by changes in the overall
density of bacteria, bacterial abundance was quanti-
fied using a broad-range bacterial primer pair. As
shown in Figure 2 (red line), fluctuation in bacterial
load across replicates and between time points was
observed. For example, in replicate 1, bacterial
abundance was highest immediately after hatching
whereas in replicate 2 hatchlings had a rather low
bacterial abundance. Thus, bacterial abundance is
not correlated with bacterial diversity, nor with
developmental age.

We next addressed the question of which bacterial
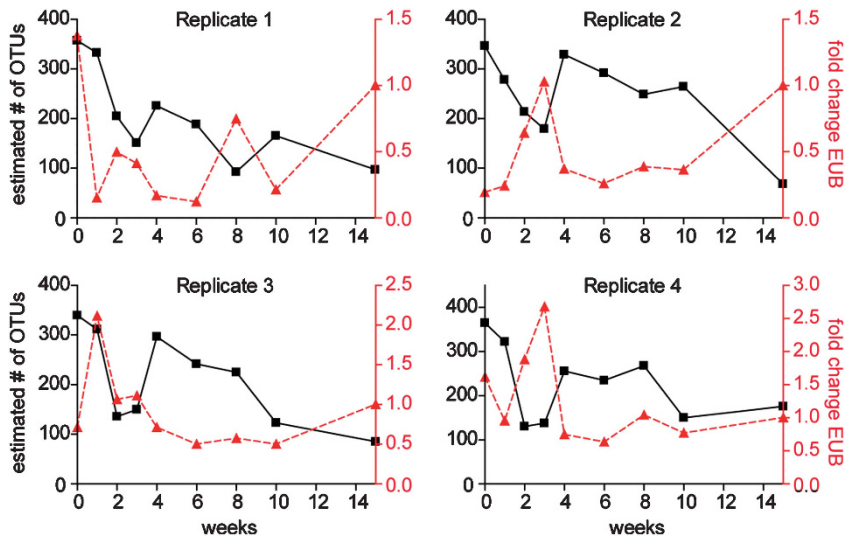species are members of the microbiota and whether

Figure 2 Dynamics of bacterial diversity and bacterial load. Estimated number of OTUs (97% sequence identity, Chao1 metric, black line) was plotted against time post hatching. Red lines indicate the relative bacterial (EUB) abundance per host cell as analyzed by quantitative PCR for the bacterial 16S gene (equilibration to *Hydra* actin, reference value 15 weeks post hatching).

membership changes during development. Sequence analysis uncovered remarkable differences between the bacterial communities in newly hatched polyps compared with adult (that is 15 weeks post hatching) animals (Figure 3a). Hatchlings were characterized by a high abundance of bacteria of the Bacteroidetes (Flavobacteria, Sphingobacteria) group, which represented about 50% of the total OTUs (Figure 3a). In addition, there was also a large number of Betaproteobacteria present in hatchlings. Other members of the bacterial community include Actinobacteria, Alphaproteobacteria and Gammaproteobacteria (Figure 3a). Interestingly, the bacterial community in polyps 15 weeks post hatching differed greatly from the composition of the community characteristic for hatchlings (Figure 3a) and resembled the previously described (Fraune *et al.*, 2010) bacterial community in clonally growing *Hydra vulgaris* (AEP) polyps.

Figure 3b shows the temporal assembly of this bacterial community (resolved at the OTU level) in four replicates at various time points after hatching. Only OTUs exceeding a relative abundance of 10% in at least one time point are shown. The assembly pattern is characterized by three distinct features. First, the bacterial composition immediately after hatching was similar in all four replicates and was characterized by a large number of *Flavobacterium sp.* (OTU 1217). Other members of the 'young' bacterial community belong to a variety of different bacterial phylotypes and include *Curvibacter* (OTU 942) (Supplementary Figure S2). Second, the first 3 weeks of assembly were characterized by a high degree of fluctuation in community composition with the presence of Burkholderiales (OTU 424) and *Acidovorax sp.* (OTU 1608) bacteria at week 1, *Curvibacter* (OTU 942) at week 2 and *Methylophilus sp.* (OTU 12), Comamonadaceae (OTU 1605) and
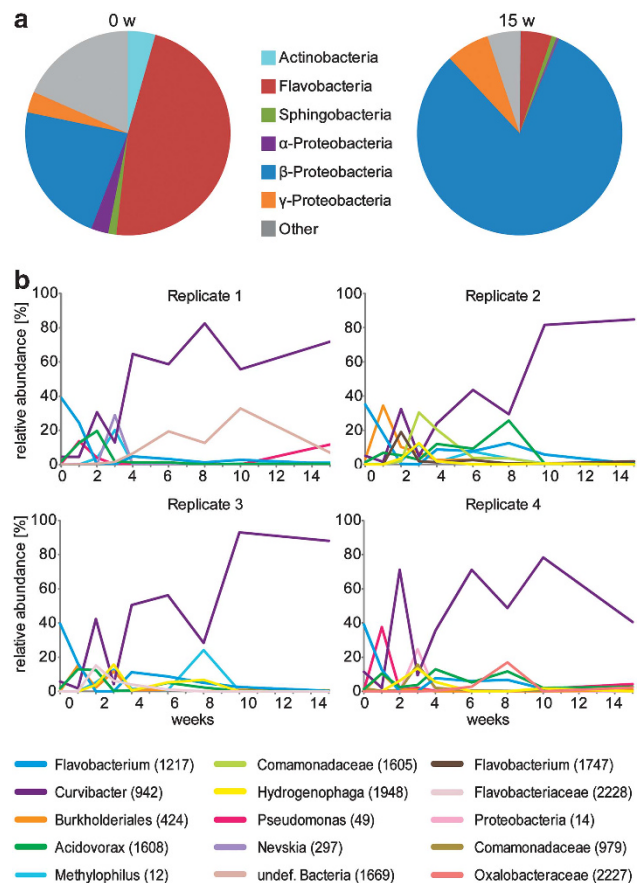

Figure 3 Dynamics in the microbiota composition. (**a**) Pie diagrams representing the bacterial community of *Hydra* polyps directly after hatching and 15 weeks post hatching, respectively. Bacterial OTUs are summarized on class level. (**b**) Relative abundances of bacterial OTUs (97% similarity) over the first 15 weeks post hatching. Only OTUs that exceed 10% in at least one sample were plotted. Note that OTU 942 (*Curvibacter sp.*) is the most abundant at week 2 in all replicates, declines again and becomes the dominating species in adult polyps.

Hydrogenophaga (OTU 1948) bacteria at week 3 in all four replicates. Third, the phase of high variability in the first weeks post hatching was replaced by the establishment of a robust bacterial composition dominated by *Curvibacter* (OTU 942) (Figure 3b). Interestingly, in all four replicates the occurrence of *Curvibacter* showed a distinct temporal pattern during assembly. Although first present at low abundance in newly hatched polyps, *Curvibacter* became the dominant member of the bacterial community for a short period of time 2 weeks post hatching. Thereafter, abundance of *Curvibacter* decreases markedly again. From week 4 on, the Betaproteobacterium *Curvibacter* became the dominant member of the bacterial community (Figure 3b; Supplementary Figure S2), which is correlated with a decrease in total bacterial diversity (Supplementary Figure S1B). As there is no general increase in bacterial load over developmental time (Figure 2), the relative increase of *Curvibacter* is because of relative changes in the community. Therefore, the host seems to offer a certain amount of niches for bacterial colonizers and over time *Curvibacter* is occupying the niches formerly used by other bacteria.

To further analyze the temporal progression of the bacterial community toward an adult-like bacterial profile, we conducted a principle coordinate analysis (Figure 4a) and calculated the average Pearson's correlation of each assembly time point (Figure 4b). As reference we used the bacterial profiles of four long-term cultures of *Hydra vulgaris* (AEP). Figure 4 A shows that the four hatchling samples cluster together, indicating a bacterial composition that substantially differs from all other samples. Principle coordinate analysis also indicates that polyps examined 1 week after hatching and three weeks after hatching have distinct bacterial communities different from those found in polyps immediately after hatching as well as from adult polyps (15 weeks post hatching). According to the principle coordinate analysis, the microbial community of polyps analyzed 4–15 weeks after hatching resembles the adult microbiota found in polyps of long-term cultures (Figure 4a). This view is supported by Pearson's correlation analysis (Figure 4b), which shows a low value immediately after hatching and in 1-week-old polyps. Two weeks post hatching, the correlation was high, indicating striking but transient resemblance to the adult-like microbial pattern. After this transient adult-like pattern the correlation drops to values similar to those found in newly hatched polyps. At 4 weeks after hatching (Figure 4b) the correlation increased and remained high in all later time points. These observations indicate that the progressive development of the adult-like microbial profile in *Hydra* encompasses a remarkable transient occurrence of the generic adult-like profile 2 weeks post hatching and a preponderance of *Curvibacter* 4 weeks after hatching.
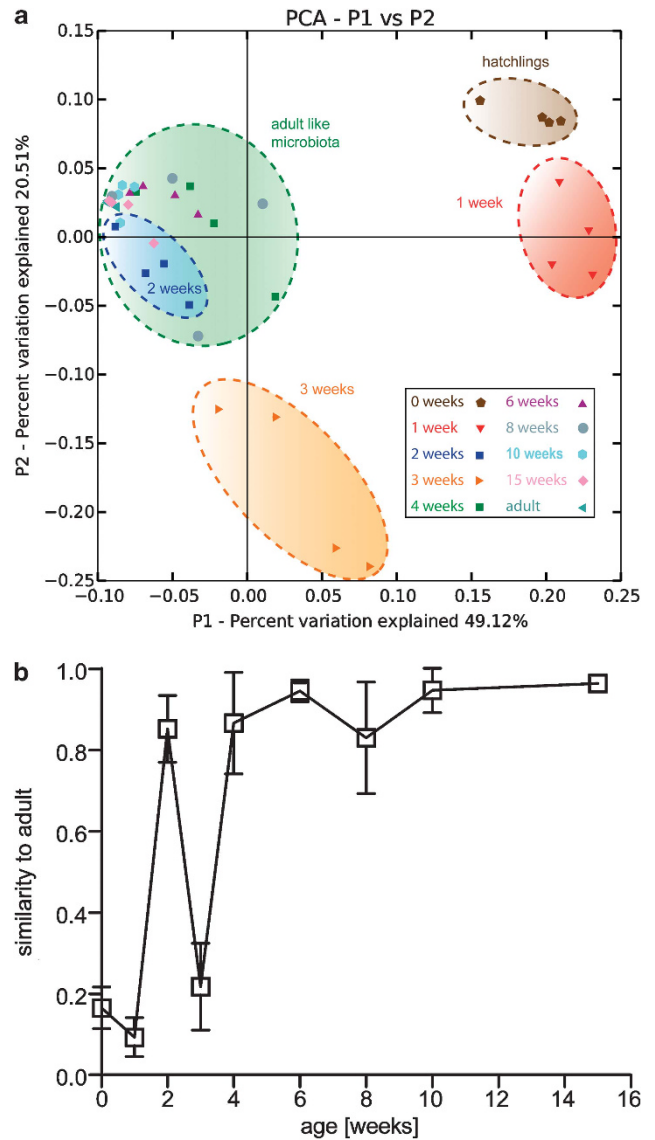
Figure 4 Temporal profile of the progression to an adult microbiota. (**a**) Principal coordinate analysis of Pearson's distances between *Hydra* microbiota at different time points post hatching. The percent variation explained by the plotted principal coordinates is indicated on the axes. The microbiota of later time points (10 weeks, 15 weeks, adult) show high similarity such that single symbols may be overlayed. (**b**) Mean Pearson's correlation between the microbiota (OTU level 97%) of each time point compared with an adult profile retrieved from four independent adult polyps (clonal propagation for 1 year). Note the peak of the Pearson's correlation at the 2-week time point.

Computing the microbial assembly pattern

Mathematical modeling is a powerful approach to understand the complexity of biological systems (Murray, 2002). Therefore, to uncover principle rules controlling the microbial assembly process in the *Hydra* metaorganism (Figure 5a), a replicator–colonizer approach was applied (Hofbauer and Sigmund, 1998). This models the temporal evolution of an interacting bacterial community in a competitive environment deterministically. This
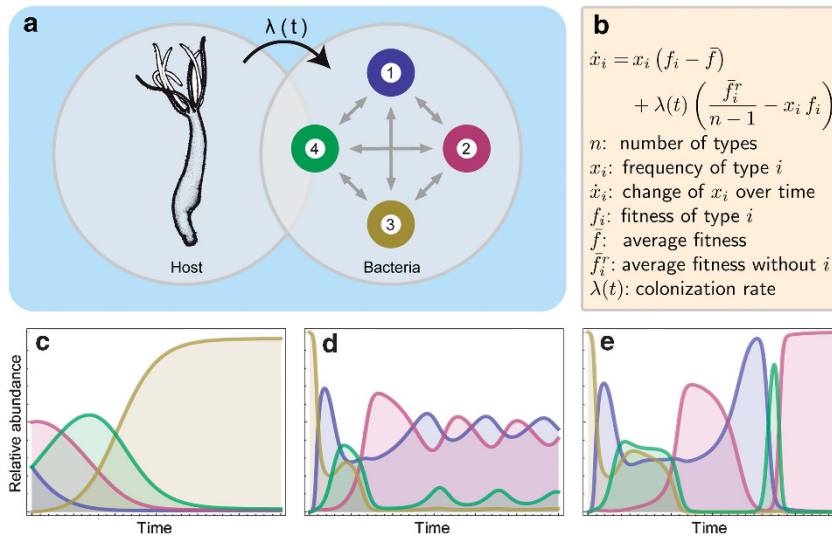
Figure 5 Mathematical modeling of the bacterial colonization process in *Hydra*. (**a**) Mathematicall model of the colonization process with $n = 4$ bacterial types, which interact pairwise and grow subject to their fitness and a colonization rate $\lambda(t)$. (**b**) The basic dynamic equation is the replicator–colonizer equation. (**c–e**) To gain qualitative understanding of the key factors of the colonization process, we follow three successive steps. First, (**c**) bacterial interactions are constant, and type-specific, the colonization rate is constant $\lambda = 0.02$. (**d**) Second, frequency-dependent interactions yield more complex behavior, for example, cyclic patterns under constant colonization rate ($\lambda = 0.02$). (**d**) Third, adding a time-decaying colonization rate, the initial oscillatory/fluctuating behavior then is damped by a factor external to the bacterial community, $\lambda(t) = 0.02e^{-t/20}$, such that the final distribution with a unique single predominant bacterial type is assumed. Thus, frequency-dependent growth rates of the bacteria are not enough to explain the dynamics, an external modulation of the colonization process is additionally required.

allowed us to qualitatively simulate the colonization dynamics based on complex interactions among bacteria and between bacteria and host. As microbial communities in *Hydra* may contain tens to hundreds of microbial species, we reduced this obviously incomprehensible complexity of community member behavior by assuming that the bacterial community only consists of four distinct members (Figure 5a). Our main assumption was that the progressive assembly of the bacterial population is restricted to pairwise interactions. The notations used in the mathematical model are defined in Figure 5b.

The mathematical analysis focused on three possible patterns of interactions within this idealized metaorganism. First, we assumed constant type-specific fitness values (constant growth and colonization rates) with competition not being dependent on the distribution of relative abundances. Here, the type with the highest growth rate wins the competition if the colonization rate is small enough. As shown in Figure 5c, the predicted colonization pattern does not agree with the qualitative pattern of the experimental data (see Figure 3b). An intermediate decline in the abundance of the final winner of the competition is not present. Next, fitness of the bacterial members of the microbiota was modeled as abundance-dependent. In this case, competition can be such that a bacterium has an advantage when it is rare, but a disadvantage when it is abundant in the community (frequency dependence). This can give rise to more complex patterns over time. The final distribution

depends on the initial distribution. The first as well as the second approach were examined by using a constant colonization rate λ (Figure 5b). As shown in Figure 5d, this can lead to an oscillatory assembly pattern resembling the observed (see Figure 3b) colonization dynamics. However, it does not capture the stable adult bacterial colonization profile of the host by a dominant bacterial species. In a third modeling step, the colonization rate was assumed to be time-dependent, that is assuming that it decays over time as the organism approaches its adult state, $\lambda(t) = \lambda_0 e^{-t/\tau}$, where τ is an environmentally or host-derived specific decay rate. In Figure 5e we show that such an environment/host-controlled colonization rate modulates the abundance-dependent competition such that an initially cyclic competition ends up in a final state dominated by a single bacterial type. Following an initial phase of oscillatory behavior, there is a transition period that sensitively depends on initial condition and on the decay rate. According to this model (see Figure 5b), the eventual winner of the microbial competition is present transiently at relatively high abundance at an earlier stage, long before a stable community with reduced bacterial diversity is reached. This modeling approach qualitatively resembles the experimental data, indicating that both inter-microbial interactions (frequency-dependent fitness) as well as environmental or host-derived factors controlling the bacterial colonization rate (λ) are important in dictating bacterial community assembly in *Hydra* polyps. Note that we do not fit any parameters to the experimental data. Instead, we infer the minimal

complexity of a mathematical model that captures crucial dynamical aspects of the colonization process. In conclusion, our study not only illustrates the feasibility of the combined *in vivo* and mathematical modeling approach to dissect the complexity of host–microbe interactions in the simple metazoan *Hydra*, but also reveals novel steps that modulate the assembly process.

Discussion

How does Hydra assemble its specific set of microbes? Animals from *Hydra* to human are colonized by a complex and species-specific microbiota (Fraune and Bosch, 2007; Ley *et al.*, 2008). In the same way that microbial communities are expected to change in different parts of a body, they are also dynamic over time. For a first understanding of the processes that control bacterial community membership in newly hatched *Hydra* polyps, we profiled the assembly of the microbiota up to 15 weeks post hatching. Our observations in four independent replicates and profiles of 36 individual polyps indicate that the adult-like microbiota arises in three stages: first the high variability and presence of numerous species, then the transient preponderance of the bacterial species, which later dominate the adult microbiota, and finally the drastic decrease of diversity and assembly to an adult-like pattern from week 4 post hatching on. Owing to the complexity of the interactions and large number of components involved, it is almost impossible to intuitively understand processes such as the assembly of the generic adult-like microbiota. We therefore complemented the *in vivo* profiling by adding a mathematical model to infer the general principles of the assembly process. One of the mathematical models (Figure 5e) not only resembles key features of the experimental data, but also makes two interesting and falsifiable predictions. First, assembly of a stable microbiota seems to require the transient preponderance of an initial member of the bacterial community, which after a characteristic decay finally becomes the stable and most abundant component of the community. Second, external (environmental or host-derived) factors given by a decaying colonization rate λ appear to be necessary to restrict oscillatory/strongly fluctuating dynamics in the bacterial population. Because environmental conditions including food, temperature and medium were highly conserved in our experimental setup, external stimuli were reduced to a minimum during the colonization process. This suggests that host factors are responsible for controlling the distinct colonization process by mediating the colonization rate λ. Thus, frequency-dependent bacteria–bacteria interactions and host control through temporal modulation of the colonization rate appear to be key features involved in dictating how the bacterial community is assembled in *Hydra* after hatching.

Interestingly, similar trends were observed recently in a study of the human infant intestinal microbiota (Palmer *et al.*, 2007). There, profiling the postnatal colonization of 14 human infants by fecal analyses showed that the intestinal microbiota is variable in infants and converges to an adult-like profile with time (Palmer *et al.*, 2007). Moreover, the Pearson's correlation shows (Palmer *et al.*, 2007) that progression toward the adult-like microbiota contains a transient state around day 5, which remarkably resembles the stable communities found in older children. Thus, in both *Hydra* and human the progressive development of the adult-like microbial profile seems to require a transient occurrence of the generic adult-like profile.

The factors and processes controlling the bacterial community assembly during ontogeny are not known. In a study comparing the microbiota of *Hydra* embryos a few hours post fertilization with adult polyps, we have previously shown that the differential colonization is reflected in differences in antimicrobial activity (Fraune *et al.*, 2010). Thus, antimicrobial peptides are capable of mediating host–microbe homeostasis (Vaishnava *et al.*, 2008; Fraune *et al.*, 2010; Salzman *et al.*, 2010; Login *et al.*, 2011) and therefore are candidates for mediating conserved progressions of certain bacteria during the ontogenetic establishment. Future efforts will be directed toward examining whether a spatially and temporally controlled expression of antimicrobial peptides contributes to the stepwise microbiota assembly after hatching from the cuticle stage. To colonize epithelial surfaces, bacteria commonly interact with glycan structures of the host glycocalyx (Hooper and Gordon, 2001). Thus, bacterial colonization of the newly hatched polyp may also be affected by this dynamic mucus layer adherent to all epithelial cells that can serve as both a physico-chemical sensor and barrier network across animal species (Moran *et al.*, 2011). Interestingly, the genome of *Curvibacter* contains a large number of ABC-transporters for sugar uptake compared with other Comamonadaceae (Chapman *et al.*, 2010). This increased potential of using the host's glycocalyx components as source of sugar for nutrition might explain the high potential of *Curvibacter* to outcompete other bacteria for the colonization of niches offered by the host.

Conclusion and perspectives
Over the last decade remarkable technical advancements have led to a better understanding of the complexity of organisms as metaorganisms and to a general picture of the interactions involved in the freshwater polyp *Hydra* (Bosch and McFall-Ngai, 2011). Precisely, how bacteria assemble in their animal host and how they contribute to the metaorganism is an exciting area of current research. We have shown here that in newly hatched *Hydra*, the microbial assembly is under complex control

mechanisms. With these insights we can now focus on identifying the underlying mechanistic processes and address questions such as: Is the remarkable variability at the onset of the assembly process host-controlled and ontogenetically fixed or a stochastic event? Does the assembly process vary between related host species? Genome-scale screens and gene-targeting experiments will have an increasing role in answering these questions and identifying the underlying molecular mechanisms. On the other hand, mathematical models of this dynamic process can lead to testable hypotheses. Collectively, the observations reported here contribute to create an integrated view of the interactions within the *Hydra* metaorganism. With regard to strikingly similar observations in human infants, it seems likely that the distinct colonization pattern described here is a common mechanistic process contributing to the composition of animal microbiota.

Acknowledgements

References

Ayres JS, Trinidad NJ, Vance RE. (2012). Lethal inflammasome activation by a multidrug-resistant pathobiont upon antibiotic disruption of the microbiota. *Nat Med* **18**: 799–806.

Bosch TC, Augustin R, Anton-Erxleben F, Fraune S, Hemmrich G, Zill H *et al.* (2009). Uncovering the evolutionary history of innate immunity: the simple metazoan Hydra uses epithelial cells for host defence. *Dev Comp Immunol* **33**: 559–569.

Bosch TC, McFall-Ngai MJ. (2011). Metaorganisms as the new frontier. *Zoology* **114**: 185–190.

Bosch TC. (2012). Understanding complex host-microbe interactions in Hydra. *Gut Microbes* **3**: 345–351.

Caporaso JG, Kuczynski J, Stombaugh J, Bittinger K, Bushman FD, Costello EK *et al.* (2010). QIIME allows analysis of high-throughput community sequencing data. *Nat Methods* **7**: 335–336.

Chapman JA, Kirkness EF, Simakov O, Hampson SE, Mitros T, Weinmaier T *et al.* (2010). The dynamic genome of Hydra. *Nature* **464**: 592–596.

Chow J, Lee SM, Shen Y, Khosravi A, Mazmanian SK. (2010). Host-bacterial symbiosis in health and disease. *Adv Immunol* **107**: 243–274.

Cilieborg MS, Boye M, Sangild PT. (2012). Bacterial colonization and gut development in preterm neonates. *Early Hum Dev* **88**(Suppl 1): S41–S49.

Drake JA. (1990). The mechanics of community assembly and succession. *J Theor Biol* **147**: 213–233.

Franzenburg S, Fraune S, Künzel S, Baines JF, Domazet-Lôso T, Bosch TC. (2012). MyD88-deficient Hydra reveal an ancient function of TLR signaling in sensing bacterial colonizers. *Proc Natl Acad Sci USA* **109**: 19374–19379.

Fraune S, Abe Y, Bosch TC. (2009). Disturbing epithelial homeostasis in the metazoan Hydra leads to drastic changes in associated microbiota. *Environ Microbiol* **11**: 2361–2369.

Fraune S, Augustin R, Anton-Erxleben F, Wittlieb J, Gelhaus C, Klimovich VB *et al.* (2010). In an early branching metazoan, bacterial colonization of the embryo is controlled by maternal antimicrobial peptides. *Proc Natl Acad Sci USA* **107**: 18067–18072.

Fraune S, Bosch TC. (2007). Long-term maintenance of species-specific bacterial microbiota in the basal metazoan Hydra. *Proc Natl Acad Sci USA* **104**: 13146–13151.

Haas BJ, Gevers D, Earl AM, Feldgarden M, Ward DV, Giannoukos G *et al.* (2011). Chimeric 16S rRNA sequence formation and detection in Sanger and 454-pyrosequenced PCR amplicons. *Genome Res* **21**: 494–504.

Hemmrich G, Anokhin B, Zacharias H, Bosch TC. (2007). Molecular phylogenetics in Hydra, a classical model in evolutionary developmental biology. *Mol Phylogenet Evol* **44**: 281–290.

Hemmrich G, Khalturin K, Boehm AM, Puchert M, Anton-Erxleben F, Wittlieb J *et al.* (2012). Molecular signatures of the three stem cell lineages in Hydra and the emergence of stem cell function at the base of multicellularity. *Mol Biol Evol* **29**: 3267–3280.

Hofbauer J, Sigmund K. (1998). *Evolutionary Games and Population Dynamics*. Cambridge University Press: Cambridge.

Hooper LV, Gordon JI. (2001). Glycans as legislators of host-microbial interactions: spanning the spectrum from symbiosis to pathogenicity. *Glycobiology* **11**: 1R–10R.

Kelly D, King T, Aminov R. (2007). Importance of microbial colonization of the gut in early life to the development of immunity. *Mutat Res* **622**: 58–69.

Koenig JE, Spor A, Scalfone N, Fricker AD, Stombaugh J, Knight R *et al.* (2011). Succession of microbial consortia in the developing infant gut microbiome. *Proc Natl Acad Sci USA* **108**(Suppl 1): 4578–4585.

Lange C, Hemmrich G, Klostermeier UC, Lopez-Quintero JA, Miller DJ, Rahn T *et al.* (2011). Defining the origins of the NOD-like receptor system at the base of animal evolution. *Mol Biol Evol* **28**: 1687–1702.

Lenhoff HM, Brown RD. (1970). Mass culture of hydra: an improved method and its application to other aquatic invertebrates. *Lab Anim* **4**: 139–154.

Ley RE, Lozupone CA, Hamady M, Knight R, Gordon JI. (2008). Worlds within worlds: evolution of the vertebrate gut microbiota. *Nat Rev Microbiol* **6**: 776–788.

Ley RE, Peterson DA, Gordon JI. (2006). Ecological and evolutionary forces shaping microbial diversity in the human intestine. *Cell* **124**: 837–848.

Login FH, Balmand S, Vallier A, Vincent-Monegat C, Vigneron A, Weiss-Gayet M *et al.* (2011). Antimicrobial peptides keep insect endosymbionts under control. *Science* **334**: 362–365.

Mao-Jones J, Ritchie KB, Jones LE, Ellner SP. (2010). How microbial community composition regulates coral disease development. *PLoS Biol* **8**: e1000345.

Martin VJ, Littlefield CL, Archer WE, Bode HR. (1997). Embryogenesis in *Hydra*. *Biol Bull* **192**: 345–363.

790

Mazmanian SK, Liu CH, Tzianabos AO, Kasper DL. (2005). An immunomodulatory molecule of symbiotic bacteria directs maturation of the host immune system. *Cell* **122**: 107–118.

Moran AP, Gupta A, Joshi L. (2011). Sweet-talk: role of host glycosylation in bacterial pathogenesis of the gastrointestinal tract. *Gut* **60**: 1412–1425.

Murray JD. (2002). *Mathematical Biology: I. An Introduction*. Springer: Berlin.

Muyzer G, de Waal EC, Uitterlinden AG. (1993). Profiling of complex microbial populations by denaturing gradient gel electrophoresis analysis of polymerase chain reaction-amplified genes coding for 16S rRNA. *Appl Environ Microbiol* **59**: 695–700.

Nyholm SV, McFall-Ngai MJ. (2004). The winnowing: establishing the squid-vibrio symbiosis. *Nat Rev Microbiol* **2**: 632–642.

Ochman H, Worobey M, Kuo CH, Ndjango JB, Peeters M, Hahn BH *et al.* (2010). Evolutionary relationships of wild hominids recapitulated by gut microbial communities. *PLoS Biol* **8**: e1000546.

Olszak T, An D, Zeissig S, Vera MP, Richter J, Franke A *et al.* (2012). Microbial exposure during early life has persistent effects on natural killer T cell function. *Science* **336**: 489–493.

Palmer C, Bik EM, DiGiulio DB, Relman DA, Brown PO. (2007). Development of the human infant intestinal microbiota. *PLoS Biol* **5**: e177.

Rawls JF, Samuel BS, Gordon JI. (2004). Gnotobiotic zebrafish reveal evolutionarily conserved responses to the gut microbiota. *Proc Natl Acad Sci USA* **101**: 4596–4601.

Salzman NH, Hung K, Haribhai D, Chu H, Karlsson-Sjoberg J, Amir E *et al.* (2010). Enteric defensins are essential regulators of intestinal microbial ecology. *Nat Immunol* **11**: 76–83.

Sandstrom J, Telang A, Moran NA. (2000). Nutritional enhancement of host plants by aphids – a comparison of three aphid species on grasses. *J Insect Physiol* **46**: 33–40.

Shin SC, Kim SH, You H, Kim B, Kim AC, Lee KA *et al.* (2011). Drosophila microbiome modulates host developmental and metabolic homeostasis via insulin signaling. *Science* **334**: 670–674.

Vaishnava S, Behrendt CL, Ismail AS, Eckmann L, Hooper LV. (2008). Paneth cells directly sense gut commensals and maintain homeostasis at the intestinal host-microbial interface. *Proc Natl Acad Sci USA* **105**: 20858–20863.

Walter J, Ley R. (2011). The human gut microbiome: ecology and recent evolutionary changes. *Annu Rev Microbiol* **65**: 411–429.

Wittlieb J, Khalturin K, Lohmann JU, Anton-Erxleben F, Bosch TC. (2006). Transgenic Hydra allow *in vivo* tracking of individual stem cells during morphogenesis. *Proc Nat Acad Sci USA* **103**: 6208–6211.

Xu J, Bjursell MK, Himrod J, Deng S, Carmichael LK, Chiang HC *et al.* (2003). A genomic view of the human-Bacteroides thetaiotaomicron symbiosis. *Science* **299**: 2074–2076.

Supplementary Information accompanies this paper on The ISME Journal website (http://www.nature.com/ismej)